NUMERICAL STUDY OF TURBULENT NATURAL CONVECTION OF NANOFLUIDS IN DIFFERENTIALLY HEATED RECTANGULAR CAVITIES

by

Zakaria LAFDAIL[a,*], Sakina EL-HAMDANI[a], Abdelaziz BENDOU[a], Karim LIMAM[b], and Bara EL-HAFAD[a]

[a] Laboratory Mechanics, Processes, Energy and Environment (LMPEE), National School of Applied Sciences, University Ibn Zohr, Agadir, Morocco
[b] LASIE, University La Rochelle, La Rochelle Cedex, France

Original scientific paper
https://doi.org/10.2298/TSCI190522444L

In this work we study numerically the turbulent natural convection of nanofluids (water + Al_2O_3/NTC/Cu) in rectangular cavities differentially heated. The objective is to compare the effect of the macro-structural aspect of the rectangular cavity and the effect of the types of nanofluids studied on the thermal exchange by turbulent natural convection in this type of geometry. Therefore, we have numerically treated the cases of these three nanofluids, for different particles volume fractions ($0 \leq \Phi \leq 0.06$) and for different form ratios of the rectangular cavity. The standard k-ε turbulence model is used to take into account the effects of turbulence. The governing equations are discretized by the finite volume method using the power law scheme which offers a good stability characteristic in this type of flow. The results are presented in the form of streamlines and isothermal lines. The variation of the average Nusselt number is calculated as a function of the types of nanoparticles, of theirs particles volume fractions, for different form ratios of the cavity, and for different Rayleigh numbers. The results show that the average Nusselt number is greater as the form ratio is large and that the effect of the use of CNT in suspension in a water prevails for voluminal fractions and large Rayleigh numbers.

Key words*: convection, natural, turbulence, nanofluid, form ratio, rectangular*

Introduction

The turbulent natural convection thermal exchange finds its application in various industrial applications such as heat exchangers in thermal power stations, cooling of electronic equipment, solar technology, safety of nuclear reactors, food and chemical industry, *etc.* So, it is important to quantify the heat exchange between a heated wall and a flowing fluid for a better design and operation of these systems especially in a context where efficiency and energy saving become one of the criteria to be respected. The intensification of thermal exchanges is based on several techniques, among them that of increasing the total exchange surface by modifying its macro-structural aspect and that of improving the thermophysical characteristics of thermal fluids. This study is part of this framework.

* Corresponding author, e-mail: zakaria.lafdaili@edu.uiz.ac.ma

The effectiveness of such processes is often limited by the thermophysical properties of the fluids used. With recent advances in nanotechnology, nanometer-sized particles can be obtained. This technological advancement gave the idea to suspend these particles in a base liquid (nanofluid) to obtain an improvement of the thermal conductivity. The amazing thermal properties of nanofluids have in fact been intensively investigated. There is, in particular, a clear increase in heat exchanges that no phenomenology can satisfactorily explain yet. This improvement in heat transfer therefore makes nanofluids a promising new technology in the context of heat transfer.

Choi and Eastman [1] improved the thermal conductivity of water by 10.7% by adding a volume fraction of 4.35% of titanium oxide (TiO_2) nanoparticles. Murshed *et al.* [2] measured the thermal conductivity of nanoparticles (TiO_2) for cylindrical nanoparticles of 40 nm, they obtain an improvement of up to 33% for a volume fraction of 5%. Ehsan *et al.* [3] studied the effect of the nanoparticle type (Cu and Al_2O_3) on the hydrodynamic and thermal characteristics of a heat transfer fluid in a square cavity with horizontal walls differentially heated. The effect of the Rayleigh number as well as that of the volume fraction of the nanofluids have also been investigated. The results obtained show that the heat transfer rate is an increasing function of the Rayleigh number and the volume fraction. Otherwise, the use of nanoparticles, of the solid metal type, has made it possible to optimize the heat exchange within the enclosure. Anish *et al.* [4] have experimentally studied the efficiency with which a nanofluid can dissipate heat in the cooling circuit of a nuclear reactor. Their results show that a combination of Al_2O_3 as a nanoparticle and therminol 55 as base fluid can considerably intensify the cooling in the reactor.

Others have studied the effect of the geometric appearance of confined enclosures on natural convection. These included the work of Morsli *et al.* [5], Oztop *et al.* [6], Flack *et al.* [7] or those of Zarrit *et al.* [8] who studied the influence of the geometry (undulations, form ratio, and inclination) of a rectangular cavity on convective heat transfer. Mahmoodi [9] studied numerically mixed convection inside rectangular enclosures filled with nanofluids with a moving bottom wall. The results highlighted the effect of geometry. Indeed, they showed that the average Nusselt number of the hot wall of tall enclosures is more that to that of the shallow enclosures. Salari *et al.* [10] studied numerically the effects of circular corners and form ratio [L/H] on entropy generation due to natural convection of nanofluid flows in rectangular cavities. The results showed that the total entropy generation increased with the increase of Rayleigh number, irreversibility coefficient, form ratio or solid volume fraction while it decreased with the increase of the corner radius.

The turbulent character of convection flows can also have positive effects [11, 12] by improving mixtures and heat and mass transfers. So, the knowledge of these phenomena can contribute to the development of strategies of control or optimization of transfers or transports of heat and mass.

In this work, we study numerically the flow of nanofluids in a rectangular cavity to highlight the effects of the nanoparticle type, Al_2O_3, Cu, and CNT, their volume fractions in the base fluid, and also the effect of form ratio on turbulent natural convection. This will allow us, in order to improve the size of rectangular cavities, to compare the effect of the type of nanoparticles and the effect of the form ratio on turbulent natural convection in this type of geometry.

Modeling and equations

The configuration studied is shown in fig. 1. It is a rectangular cavity filled with water containing different particles volume fractions of (Al_2O_3, CNT, or Cu). The cavity is

formed by a left vertical wall at a hot temperature, a straight vertical wall maintained at a cold temperature and two horizontal walls considered adiabatic.

The thermophysical properties of the nanofluids are constant, except for the variation of the density which is estimated by the Boussinesq approximation. The thermophysical properties of the pure fluid and the nanoparticles studied are summarized in tab. 1.

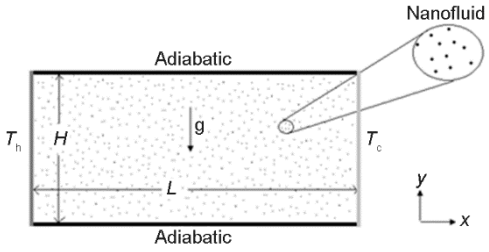

Figue 1. Geometry and limit conditions of the configuration studied

Table 1. Thermophysical properties of water and nanoparticles for temperatures between 293 K and 303 K

	Pr	ρ [kgm^{-3}]	Cp [Jkg^{-1}K^{-1}]	k [Wm^{-1}K^{-1}]	β [10^{-5}k^{-5}]
Pure water	4.8	997	4186	0.61	27
Cu	–	8933	385	400	1.67
Al_2O_3	–	3970	765	40	0.85
CNT	–	1800	720	6600	0.1

To account for the effects of turbulence, the k-ε model is used. Therefore, the governing equations written in the Cartesian co-ordinate system (x, y) are:

– Equation of continuity:

$$\frac{\partial \rho}{\partial t} + \frac{\partial (\rho u)}{\partial x} + \frac{\partial (\rho v)}{\partial y} = 0 \tag{1}$$

– Momentum equation in the x-direction:

$$\rho_{\mathrm{nf}} \frac{\partial u}{\partial t} + \rho_{\mathrm{nf}} u \frac{\partial u}{\partial x} + \rho_{\mathrm{nf}} v \frac{\partial u}{\partial y} = -\frac{\partial p}{\partial x} + \frac{\partial}{\partial x} \cdot$$
$$\cdot \left\{ [\mu_{\mathrm{nf}} + (\mu_{\mathrm{t}})_{\mathrm{nf}}] \left(2 \frac{\partial u}{\partial x} \right) \right\} + \frac{\partial}{\partial y} \left\{ [\mu_{\mathrm{nf}} + (\mu_{\mathrm{t}})_{\mathrm{nf}}] \left(\frac{\partial u}{\partial y} + \frac{\partial v}{\partial x} \right) \right\} \tag{2}$$

– Momentum equation in the y-direction:

$$\rho_{\mathrm{nf}} \frac{\partial v}{\partial t} + \rho_{\mathrm{nf}} u \frac{\partial v}{\partial x} + \rho_{\mathrm{nf}} v \frac{\partial v}{\partial y} = -\frac{\partial p}{\partial y} + \frac{\partial}{\partial y} \left\{ [\mu_{\mathrm{nf}} + (\mu_{\mathrm{t}})_{\mathrm{nf}}] \left(2 \frac{\partial v}{\partial y} \right) \right\} +$$
$$+ \frac{\partial}{\partial x} \left\{ [\mu_{\mathrm{nf}} + (\mu_{\mathrm{t}})_{\mathrm{nf}}] \left(\frac{\partial u}{\partial y} + \frac{\partial v}{\partial x} \right) \right\} + \mathrm{g} \rho_{\mathrm{nf}} \beta_{\mathrm{nf}} (T - T_{\mathrm{ref}}) \tag{3}$$

– Thermal energy equation:

$$\rho_{\mathrm{nf}} \frac{\partial T}{\partial t} + \rho_{\mathrm{nf}} u \frac{\partial T}{\partial x} + \rho_{\mathrm{nf}} v \frac{\partial T}{\partial y} = \frac{\partial}{\partial x} \left\{ \left[\frac{\mu_{\mathrm{nf}}}{\mathrm{Pr}_{\mathrm{nf}}} + \frac{(\mu_{\mathrm{t}})_{\mathrm{nf}}}{\sigma_t} \right] \frac{\partial T}{\partial x} \right\} + \frac{\partial}{\partial y} \left\{ \left[\frac{\mu_{\mathrm{nf}}}{\mathrm{Pr}_{\mathrm{nf}}} + \frac{(\mu_{\mathrm{t}})_{\mathrm{nf}}}{\sigma_t} \right] \frac{\partial T}{\partial y} \right\} \tag{4}$$

– Turbulent kinetic energy equation:

$$\rho_{\mathrm{nf}}\frac{\partial k}{\partial t}+\rho_{\mathrm{nf}}u\frac{\partial k}{\partial x}+\rho_{\mathrm{nf}}v\frac{\partial k}{\partial y}=\frac{\partial}{\partial x}\left\{\left[\mu_{\mathrm{nf}}+\frac{(\mu_{\mathrm{t}})_{\mathrm{nf}}}{\sigma_k}\right]\frac{\partial k}{\partial x}\right\}+\frac{\partial}{\partial y}\left\{\left[\mu_{\mathrm{nf}}+\frac{(\mu_{\mathrm{t}})_{\mathrm{nf}}}{\sigma_k}\right]\frac{\partial k}{\partial y}\right\}+$$

$$+(P_k)_{\mathrm{nf}}+(G_k)_{\mathrm{nf}}-\rho_{\mathrm{nf}}\varepsilon \tag{5}$$

– Equation for the rate of energy dissipation:

$$\rho_{\mathrm{nf}}\frac{\partial \varepsilon}{\partial t}+\rho_{\mathrm{nf}}u\frac{\partial \varepsilon}{\partial x}+\rho_{\mathrm{nf}}v\frac{\partial \varepsilon}{\partial y}=\frac{\partial}{\partial x}\left\{\left[\mu_{\mathrm{nf}}+\frac{(\mu_{\mathrm{t}})_{\mathrm{nf}}}{\sigma_\varepsilon}\right]\frac{\partial \varepsilon}{\partial x}\right\}+\frac{\partial}{\partial y}\left\{\left[\mu_{\mathrm{nf}}+\frac{(\mu_{\mathrm{t}})_{\mathrm{nf}}}{\sigma_\varepsilon}\right]\frac{\partial \varepsilon}{\partial y}\right\}+$$

$$+\left\{C_{\varepsilon 1}f_1[(P_k)_{\mathrm{nf}}+C_{\varepsilon 3}(G_k)_{\mathrm{nf}}]-\rho_{\mathrm{nf}}C_{\varepsilon 2}f_2\varepsilon\right\}\frac{\varepsilon}{k} \tag{6}$$

where $(P_k)_{\mathrm{nf}}$ represents the stress production and is calculated as:

$$(P_k)_{\mathrm{nf}}=(\mu_{\mathrm{t}})_{\mathrm{nf}}\left[2\left(\frac{\partial u}{\partial x}\right)^2+2\left(\frac{\partial v}{\partial y}\right)^2+\left(\frac{\partial u}{\partial y}+\frac{\partial v}{\partial x}\right)^2\right] \tag{7}$$

and $(G_k)_{\mathrm{nf}}$ is the buoyancy term, and is defined as:

$$(G_k)_{\mathrm{nf}}=\frac{(\mu_t)_{\mathrm{nf}}}{\sigma_T}\mathrm{g}\beta_{\mathrm{nf}}\frac{\partial T}{\partial y} \tag{8}$$

The Prandtl number is calculated:

$$\mathrm{Pr}_{\mathrm{nf}}=\frac{Cp_{\mathrm{nf}}\mu_{\mathrm{nf}}K_{\mathrm{eff,f}}}{Cp_{\mathrm{f}}\mu_{\mathrm{f}}K_{\mathrm{eff,nf}}}\mathrm{Pr} \tag{9}$$

The following formulas were used to compute the thermal and physical properties of the nanofluids under consideration:

The eddy viscosity is calculated:

$$(\mu_t)_{\mathrm{nf}}=\rho_{\mathrm{nf}}C_\mu f_\mu\frac{k^2}{\varepsilon} \tag{10}$$

where μ_{nf} is the dynamic viscosity of the nanofluid defined by the Brinkman model [13]:

$$\mu_{\mathrm{nf}}=\frac{\mu_f}{(1-\Phi_{\mathrm{p}})^{2.5}} \tag{11}$$

where $K_{\mathrm{eff,nf}}$ is the effective thermal conductivity of the nanofluid defined by the Maxwell-Garnetts model [14]:

$$K_{\mathrm{eff,nf}}=K_{\mathrm{eff,f}}\left[\frac{(K_{\mathrm{eff,p}}+2K_{\mathrm{eff,f}})-2\Phi(K_{\mathrm{eff,f}}+K_{\mathrm{eff,p}})}{(K_{\mathrm{eff,p}}+2K_{\mathrm{eff,f}})+\Phi(K_{\mathrm{eff,f}}+K_{\mathrm{eff,p}})}\right] \tag{12}$$

Equations (13)-(15) are general relationships used to compute the density, the coefficient of thermal expansion and the heat capacity for a classical two-phase mixture [15].

$$\rho_{\mathrm{nf}} = (1-\Phi)\rho_{\mathrm{f}} + \Phi\rho_{\mathrm{p}} \tag{13}$$

$$\beta_{\mathrm{nf}} = (1-\Phi)\beta_{\mathrm{f}} + \Phi\beta_{\mathrm{p}} \tag{14}$$

$$Cp_{\mathrm{nf}} = (1-\Phi)Cp_{\mathrm{f}} + \Phi Cp_{\mathrm{p}} \tag{15}$$

The empirical constants were recommended by Launder and Spalding [16] is listed in tab. 2.

Table 2. The values of the constants in the *k*-ε model

C_μ	$C_{\varepsilon 1}$	$C_{\varepsilon 2}$	σ_k	σ_ε	f_1	f_2	f_μ
0.09	1.44	1.92	1.0	1.33	1.0	1.0	1.0

The expression of $C_{\varepsilon 3}$ suggested by Henkes *et al.* [17] is used:

$$C_{\varepsilon 3} = \tanh\left(\frac{u}{v}\right) \tag{17}$$

All physical properties were estimated at the average temperature:

$$T_{\mathrm{ref}} = \frac{T_{\mathrm{h}} + T_{\mathrm{c}}}{2} \tag{18}$$

The Rayleigh number is defined:

$$\mathrm{Ra} = \frac{\rho_{\mathrm{nf}}^2 \mathrm{g}\beta_{\mathrm{nf}}\Delta T H^3}{\mu_{\mathrm{nf}}^2}\mathrm{Pr}_{\mathrm{nf}} \tag{19}$$

The average Nusselt number, $\mathrm{Nu}_{\mathrm{av}}$, of the hot wall is expressed:

$$\mathrm{Nu}_{\mathrm{av}} = -\frac{K_{\mathrm{eff,f}}}{HK_{\mathrm{eff,nf}}}\int_0^H \left(\frac{\partial T}{\partial x}\right)_{x=0} \mathrm{d}x \tag{20}$$

The form ratio of the cavity is defined:

$$FR = \frac{L}{H} \tag{21}$$

Numerical resolution and code validation

To numerically solve partial differential eqs. (1)-(6), we proceeded to their discretizations in order to obtain a system of algebraic equations whose resolution allows us to determine the fields of all the variables of the problem considered. The finite volume method was adopted to accomplish this discretization and the use of the SIMPLE algorithm for pressure correction.

The computational domain is subdivided into a finite number of elementary subdomains, called control volumes. Each of these includes a node called main node, as shown in fig. 2.

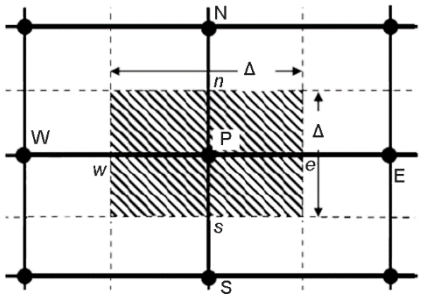

Figure 2. Bi-dimensional control volume

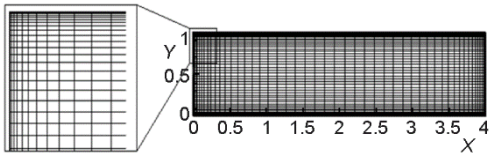

Figure 3. Refined uniform mesh near the walls

For a main node P, points E and W (East and West) are neighbors in the *x*-direction, while N and S (North and South) are those in the *y*-direction. The control volume surrounding P is shown by broken lines. The faces of the control volume are located at the points e and w in *x*-direction, n and s in the *y*-direction.

Turbulent flows are significantly influenced near walls. Indeed, in areas very close to the walls, the viscosity effects reduce the fluctuations of the tangential velocities. Therefore, to model the flows near the walls, we used a refined uniform mesh near the walls, as shown in fig. 3.

To study the influence of the mesh, we calculated the average Nusselt number for different grids and for different forms ratio. The results obtained for cavities filled with pure water and for a Rayleigh number of 10^9 are presented in tab. 3.

From tab. 3, it appears that the grids 120 × 120, 200 × 100, 300 × 100, and 320 × 80 are fine enough to perform the numerical simulations successively for the form ratios 1-4.

Table 3. Validation of the grid for different forms ratio

FR = 1	Grid	60×60	80×80	100×100	120×120	140×140
	Nu_{av}	53.70	54.06	54.22	54.34	54.37
	Rate of difference of the Nu_{av}	–	0.67%	0.29%	0.22%	0.05%
FR = 2	Grid	120×60	160×80	200×100	240×120	–
	Nu_{av}	53.47	53.68	53.80	53.85	–
	Rate of difference of the Nu_{av}	–	0.39%	0.22%	0.09%	–
FR = 3	Grid	180×60	240×80	300×100	360×120	–
	Nu_{av}	53.07	53.25	53.37	53.42	–
	Rate of difference of the Nu_{av}	–	0.33%	0.22%	0.009%	–
FR = 4	Grid	240×60	320×80	360×100	–	–
	Nu_{av}	52.63	52.75	52.89	–	–
	Rate of difference of the Nu_{av}	–	0.23%	0.17%	–	–

We used the finite volume method and the *power law* scheme for the discretization of the equations of momentum and energy. The finite volume technique essentially comprises the following steps:

– the division of the calculation domain into control volumes,
– integral formulation of partial differential equations,
– writing algebraic equations to the nodes of the mesh, and

– resolution of the algebraic system of nonlinear equation obtained.

The numerical resolution of the problem was carried out by an elaborate numerical code. The dynamic and thermal fields are calculated iteratively until the following convergence criterion is satisfied: the maximum residual value of mass, momentum, and heat energy be less than 10^{-6}.

To validate the current numerical method, we compared the average Nusselt number values calculated on the cold wall of a cavity filled with air with those found by Bairi *et al.* [18], Marakos *et al.* [19], and Dixit *et al.* [20]. The details of the calculation of the average Nusselt number for Rayleigh number values ($10^7 \leq Ra \leq 10^9$) ($10^7 \leq Ra \leq 10^9$) are presented in tab. 4.

Table 4. Comparison of average Nusselt number values with literature works

Ra	Present paper	[18]	[19]	[20]
10^7	16.47	16.073	–	16.8
10^8	30.10	31.339	32.3	30.5
10^9	54.37	–	60.1	57.4

It is clear that the results of our code are in good agreement with those proposed by Bairi *et al.* [18], Marakos *et al.* [19], and Dixit *et al.* [20].

We also present the variations of the vertical velocity and the variations of the temperature at half-height of the cavity as shown in figs. 4 and 5. The values of speed are almost confused with those of experience. Moreover, the temperature values show good agreement with those of the experiment. These are slightly higher than those calculated numerically in the middle of the cavity.

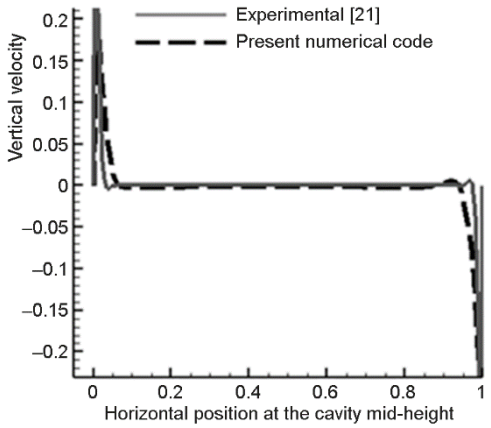

Figure 4. Variation of the vertical velocity as a function of *X* at mid-height of the cavity

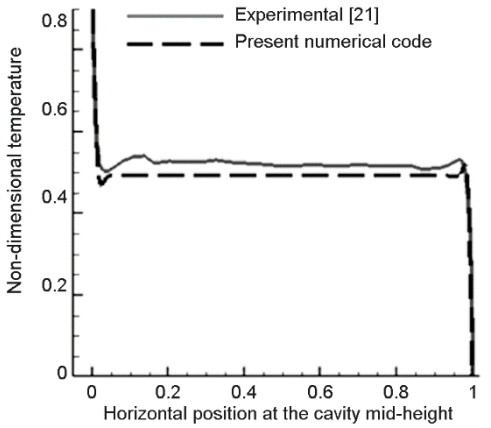

Figure 5. Variation of the temperature as a function of *X* at mid-height of the cavity

Results and discussions

Figures 6 and 7 successively represent the isotherms contours and streamlines of the nanofluid (water + Al_2O_3, $\Phi = 0.04$) for Rayleigh numbers ranging from 10^7 to 10^9 in a rectangular cavity (FR = 2) differentially heated.

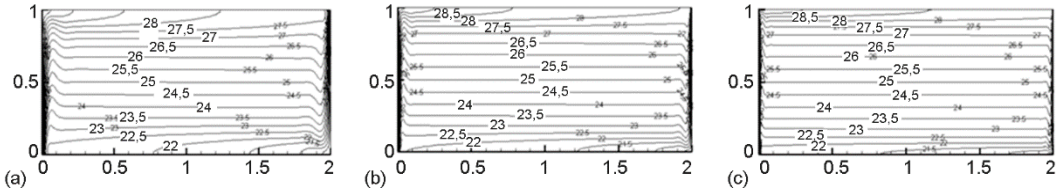

Figure 6. Isotherms contours of the nanofluid (water + Al_2O_3, Φ = 0.04) in a rectangular cavity (FR = 2) for (a) Ra = 10^7 (b) Ra = 10^8, and (c) Ra = 10^9

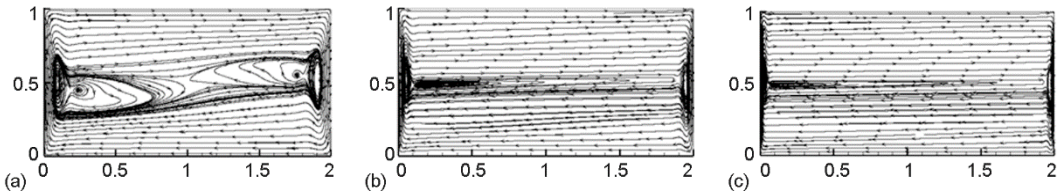

Figure 7. Streamlines of the nanofluid (water + Al_2O_3, Φ = 0.04) in a rectangular cavity (FR = 2) for (a) Ra = 10^7 (b) Ra = 10^8, and (c) Ra = 10^9

The isotherms contours and the streamlines successively shown in figs. 6 and 7 are marked by horizontal stratification and are all the more stagnant inside the cavity as the Rayleigh number is large, which means that the heat of the transfer is largely done by convection.

We also see that the gradients of temperature and velocity become steeper near the vertical walls for high Rayleigh numbers, which shows that most of the turbulent flow occurs along the vertical sides of the cavity.

The average Nusselt number along the cold wall is shown in figs. 8(a)-8(c) for different Rayleigh number, for different types of nanoparticles and for different form ratios of the cavity.

From the results, it is clear that the form ratio of the rectangular cavity greatly influences convective heat exchange. Indeed, the heat exchange surface decreases for high form ratios, which explain the decrease in the average Nusselt number for reports of shape of larger and larger. We can also see that the effect of the type of nanoparticle is even greater than the number of Rayleigh is large. fig. 8(c) shows that for Ra = 10^9 and for $\Phi > 0.04$, the curves representing the mean Nusselt number as a function of the volume fractions of the three nanoparticles (Al_2O_3, NTC, and Cu) and for the four form ratios (1-4) are distinguished, in particular, for those of nanofluid based NTC. This means that the NTC nanoparticles significantly improve the thermophysical properties of the fluid in turbulent flow. Therefore, the use of NTC-based fluids can significantly improve the design of heat exchange systems to better optimize sizing and development of thermal management strategies.

Conclusions

The present work has numerically studied the effects of nanoparticles (Al_2O_3, CNT, and Cu) and shape ratio on the rate of heat transfer by turbulent natural convection inside a rectangular cavity. Numerical simulations that are made for different Rayleigh numbers (10^7, 10^8, and 10^9) for different form ratios and for different volume fractions of the nanoparticles have shown that:

- The Nusselt number increases regularly for increasing volume fractions. Indeed, the suspensions of nanoparticles in the water significantly modify the thermal conductivity of the solution which improves the heat transfer.

- The use of CNT suspended in water allows to make an improvement of the thermal performances that is much more important to the solution compared to the use of nanoparticles of alumina or copper.
- The effect of the type and the volume fraction of the nanoparticles on the value of the Nusselt number are even greater than the Rayleigh number is large.
- The form ratio greatly influences the number of Nusselt. Indeed, the exchange surface increases for decreasing form report, which intensifies the heat transfer by natural convection.

The results obtained clearly show that the use of carbon-based nanofluids and the macro-structural aspect of the cavity can considerably influence the turbulent natural convective heat transfer in this type of geometry.

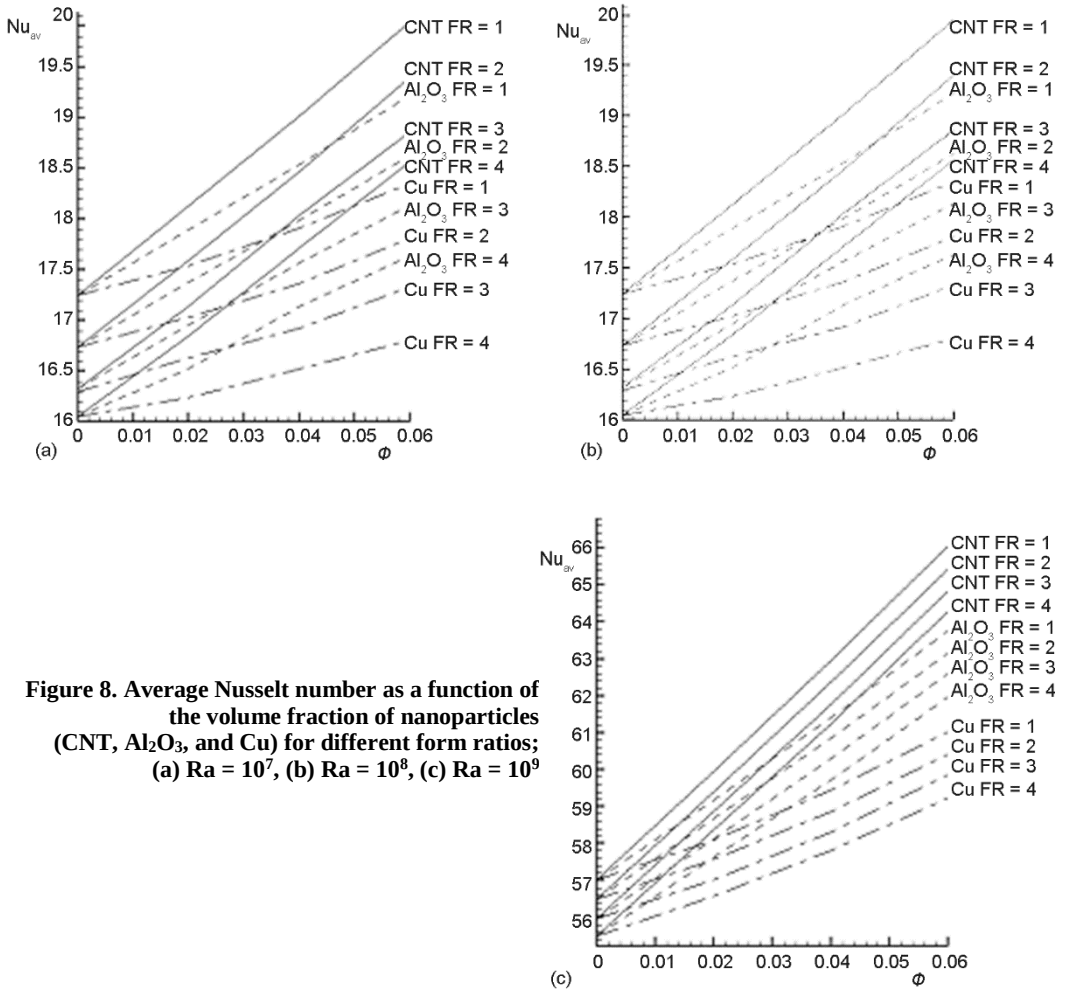

Figure 8. Average Nusselt number as a function of the volume fraction of nanoparticles (CNT, Al_2O_3, and Cu) for different form ratios; (a) Ra = 10^7, (b) Ra = 10^8, (c) Ra = 10^9

Acknowledgment

I am grateful to all of those with whom I have had the pleasure to work during this and other related projects. Each of the members of my Dissertation Committee has provided me extensive personal and professional guidance and taught me a great deal about both scientific research and life in general. I would especially like to thank Dr. Sakina El Hamdani, the chairman of my committee. As my teacher and mentor, he has taught me more than I could ever give him credit for here.

I would like to thank my parents, whose love and guidance are with me in whatever I pursue. They are the ultimate role models. Most importantly, I wish to thank my loving and supportive wife, Naoual, and my son, Yahya, who provide unending inspiration.

Nomenclature

Cp – specific heat at constant pressure, [Jkg^{-1}K^{-1}]
FR – form ratio
g – gravity acceleration, [ms^{-2}]
H – cavity height, [m]
k – turbulent kinetic energy, [m^{2}s^{-2}]
K_{eff} – effective thermal conductivity
L – cavity width, [m]
Nu – Nusselt number
Pr – Prandtl number
p – pressure, [Pa]
Ra – Rayleigh number
T – temperature, [K]
t – time, [s]
u, v – velocity components, [ms^{-1}]
x, y – Cartesian co-ordinates, [m]

Greek symbols

α – thermal diffusivity, [m^{2}s^{-1}]
β – volumetric coefficient of thermal expansion, [K^{-1}]
ε – dissipation rate of turbulent kinetic energy
μ – dynamic viscosity, [Nsm^{-2}]
ν – kinematic viscosity, [m^{2}s^{-1}]
ρ – density, [kgm^{-3}]
σ_k, σ_t σ_ε – numbers of turbulent Prandtl of k, t and ε
Φ – particle volume fraction

Subscripts

av – average
c – cold
f – fluid
h – hot
nf – nanofluid
p – nanoparticle
ref – reference
t – turbulent

References

[1] Choi, S. U. S., Eastman, J. A., Enhancing Thermal Conductivity of Fluids with Nanoparticules, *Developments and Applications of Non-Newtonian Flows, FED-Vol. 231/MD-Vol. 66* (1995), Oct., pp. 99-105
[2] Murshed, S. M. S., *et al.*, Thermal Conductivity of Nanoparticle Suspensions, *Proceedings*, Conference on Emergeing Technologies – Nanoelectronics, Singapore, Singapore, 2007
[3] Ehsan, F., *et al.*, Lattice Boltzmann Simulation of Natural Convection Heat Transfer in Nanofluids, *Int. J. Thermal Sciences, 52* (2012), Feb., pp. 137-144
[4] Anish, M., *et al.,* Experimental Study of Heat Transfer Through Cooling Water Circuit in a Reactor Vault by uSing Al_2O_3 Nanofluid, *Thermal Sciences, 22* (2018), 2, pp. 1149-1161
[5] Morsli, S., *et al.,* Influence of Aspect Ratio on the Natural Convection and Entropy Generation in Rectangular Cavities with Wavy-Wall, *ScienceDirect Energy Procedia, 139* (2017), Dec., pp. 29-36
[6] Oztop, H. F., *et al.*, Natural convection in wavy enclosures with volumetric heat sources, *International Journal of Thermal Sciences, 50* (2011), 4, pp. 502-514
[7] Flack, R. D., *et al.*, The Measurement of Natural Convective Heat Transfer in Triangular Enclosures, *J. Heat Transfer, Trans, ASME, 101* (1979), 7, pp. 648-654
[8] Zarrit, R., *et al.,* Natural Convection in an Inclined Rectangular Cavity of Different Form Reports (in French), *Revue des Energies Renouvelables, 19* (2016), 1, pp. 97-109
[9] Mahmoodi, M., Mixed Convection Inside Nanofluid Filled Rectangular Enclosures with Movingbottom wall, *Thermal Science, 15* (2011), 3, pp. pp. 889-903
[10] Salari, S., *et al.,* Effects of Circular Corners and Aspect-Ratio on Entropy Generation Due to Natural Convection of Nanofluid Flows in Rectangular Cavities, *Thermal Science, 19* (2015), 5, pp. 1621-1632

[11] Mebrouk, R., *et al.,* Numerical Study of Natural Turbulent Convection of Nanofluids in a Tall Cavity hEated from Below, *Thermal Science, 20* (2016), 6, pp. 2051-2064
[12] Salari, M., *et al.,* 3D Numerical Analysis of Natural Convection and Entropy Generation within Tilted Rectangular Enclosures Filled with Stratified Fluids of MWCNTs/Water Nanofluid and Air, *Journal of the Taiwan Institute of Chemical Engineers, 80* (2017), Nov., pp. 621-639
[13] Brinkman, H. C., The Viscosity of Concentrated Suspensions and Solutions, *J. Chem. Phys., 20* (1952), pp. 571-581
[14] Maxwell, J. C., *A Treatise on Electricity and Magnetism*, Clarendon Press, Oxford, UK, 1891
[15] Pak, B. C., Cho, Y. I., Hydrodynamic and Heat Transfer Study of Dispersed Fluids with Submicron Metallic Oxide Particles, *Exp. Heat Transfer, 11* (1998). 2, pp. 151-170
[16] Launder, B. E., Spalding, D. B., The Numerical Computation of Turbulent Flows, *Comput. Methods Appl. Mech. Eng., 3* (1974), 2, pp. 269-289
[17] Henkes, *et al.,* Comparison of the Standard Case for Turbulent Natural Convection in a Square Enclosure, *Proceedings,* Turbulent Natural Convection in Enclosures: A Computational and Experimental Benchmark Study (eds. Henkes R. A. W. M. and Hoogendoorn, C. J.), Delft, The Netheriands, 1992, pp. 185-213
[18] Bairi, A., *et al.,* Nusselt-Rayleigh Correlations for Design of Industrial Elements Experimental and Numerical Investigation of Natural Convection in Tilted Square Air Filled Enclosures, *Energy Conversion and Management, 49* (2008), 4, pp. 771-782
[19] Marakos, N. C., *et al.* Laminar and Turbulent Natural Convection in an Enclosed Cavity, *Int. J. Heat Mass Transfer, 27* (1984), 5, pp. 755-772
[20] Dixit, H. N., *et al.,* Simulation of high Rayleigh Number Convection in a Square Cavity Using the Lattice Boltzmann Method, *Int. J. Heat and Mass Transfer, 49* (2006), 3-4, pp. 727-739
[21] Ampofo, *et al.,* Experimental Benchmark Data for Turbulent Natural Convection in an Air Filled Square Cavity, *Int. J. Heat Mass Transfer, 46* (2003), 19, pp. 3551-3572

Paper submitted: May 22, 2019
Paper revised: September 19, 2019
Paper accepted: November 20, 2019